Thesis for the Degree of Master of Engineering

Characterization of astaxanthin for proliferation and osteogenic potential of mesenchymal stem cells in tissue-engineered scaffolds

By

Bo Young Choi

Interdisciplinary Program of Biomedical Mechanical & Electrical Engineering

The Graduate School

Pukyong National University

February 2020

Characterization of astaxanthin for proliferation and osteogenic potential of mesenchymal stem cells in tissue-engineered scaffolds

조직공학 지지체 내 중간엽 줄기 세포 증식 및 골형성 분화를 위한 아스타잔틴의 특성에 대한 연구

Advisor: Prof. Seung Yun Nam

by

Bo Young Choi

A thesis submitted in partial fulfillment of the requirements

for the degree of

Master of Engineering

in Interdisciplinary Program of Biomedical Mechanical & Electrical Engineering,

The Graduate School

Pukyong National University

February 2020

Characterization of astaxanthin for proliferation and osteogenic potential of mesenchymal stem cells in tissue-engineered scaffolds

A dissertation

by

Bo Young Choi

Approved by:

(Chairman) Sang-Hyug Park

(Member) Joong Ho Shin

(Member) Seung Yun Nam

February 21, 2020

조직공학 지지체 내 중간엽 줄기세포 증식 및 골형성 분화를 위한 아스타잔틴의 특성에 대한 연구

최 보 영

부경대학교 대학원 의생명기계전기융합공학협동과정

요 약

최근 조직 공학 및 재생의학 분야에서 생체 적합성을 보유한 해양유래 물질들이 각광받고 있다. 아스타잔틴은 미세조류나 갑각류 등 자연계에 널리 분포하고 있는 카로테노이드 물질 중 하나이다. 또한, 아스타잔틴은 분자구조에 의해서 생성된 활성산소를 막는 항산화 특성과 항염증, 항암, 항당뇨 등 다양한 생리활성 효과를 지닌 물질로 알려져 있다. 또한, 약리학, 치료 및 화장품 등 다양한 분야에서 우수한 기능성 물질로 평가되고 있다.

본 연구에서는 이러한 아스타잔틴의 특성을 이용하여 지방유래 줄기세포의 증식뿐만 아니라 골분화 유도를 위한 연구를 진행하였다. 줄기세포의 증식을 보는 실험에서는 생체 모사 환경을 체외에서 조성하기 위하여 자외선에 의해 경화되는 gelatin-methacryoyl (GelMA)를 세포 지지체로 사용하여 실험을 진행하였다. 화학적, 기계적 분석을 통해 세포지지체의 특성을 확인하고, 생물학적 실험을 통해 아스타잔틴이 줄기세포 증식에 대한 영향을 정량적으로 분석하였다. 또한, polycaprolactone (PCL)을 기반으로 한 세포지지체를 제작해 GelMA와 아스타잔틴의 혼합물을 소수성인 PCL위에 코팅하여 아스타잔틴의 골분화 유도능을 확인하는 연구를 진행하였다. 본 연구를 통해 아스타잔틴은 3D 배양 시스템 및 다양한 조직 공학 응용분야에 유용한 물질이 될 수 있다는 것을 확인하였다.

Table of contents

List of tables

List of figures

1. Introduction

Recently, marine-derived materials are of greater interest because of bioactivity, availability and economic viability in tissue engineering applications [1]. Astaxanthin (3,-3'-dihydroxy-β, β-carotene-4, 4' -dione) can be obtained from marine microorganisms and species such as the microalgae *Haematococcus pluvialis*, *Euphausia superba,* and *Phaffia rhodozyma* (figure. 1). As one of red carotenoid pigments, it constitutes unique structures of the ketone, hydroxyl groups and the polyene chains that help to convert unstable electrons into a stable state (figure. 2).

It has outstanding anti-cancer, anti-diabetic properties compared to other antioxidant carotenoids. Astaxanthin can be used for various fields of applications such as pharmacological, therapeutic, and cosmetic parts. Recently, studies reported that not only can astaxanthin improve stem cell potency through the PI3K and MEK signaling pathways but also it can enhance the differentiation of adipose-derived mesenchymal stem cells into oligodendrocytes, osteoblasts, chondrocytes, and adipocytes [2-8]. These studies demonstrated the feasibility of the use of astaxanthin in various applications of tissue engineering and regenerative medicine.

The encapsulation of living cells into biomaterials helps a uniform interaction of bioactive metabolite with native cells providing a close resemblance of the *in vivo* microenvironment. Gelatin methacryloyl (GelMA) has been widely used to create three-dimensional cell-laden systems and create *in vivo* mimicry in tissue engineering applications. Gelatin modified materials has RGD sequences (arginine-glycine-aspartic

acid) which provide sites for cell attachment and sequences of matrix metalloproteinase (MMP) for biodegradability. It also provides superior biocompatibility and easily tunable physical properties. As a photopolymer, it forms covalently crosslinked hydrogels when exposed to ultraviolet (UV) or visible light in the presence of photoinitiators such as the Lithium phenyl-2,4,6-trimethylbenzoylphosphinate (LAP) and 2-hydroxy-4'-(2-hydroxyethoxy)-2-methylpropiophenone (Irgacure 2959) [9-16]. In tissue engineering and regenerative medicine, many studies have shown that stem cells encapsulated in three-dimensional GelMA scaffolds can be used for the treatment of various disease and have exhibited positive impacts (figure. 3) [17-22].

In this study, the goal is to study the influence of astaxanthin-incorporated GelMA hydrogels in three-dimensional environment on the proliferative potential of adipose-derived stem cells. Firstly, astaxanthin was tested to access the cellular proliferation and gene expression in two-dimensional environment using alamar blue assay and RT-PCR. Moreover, GelMA scaffolds with and without astaxanthin were fabricated (figure. 4) and physically and chemically characterized by NMR analysis, rheological assessment, and swelling ratio test. Finally, cellular proliferation and viability in the astaxanthin incorporated GelMA hydrogels were assessed using alamar blue assay and confocal imaging with live/dead assay.

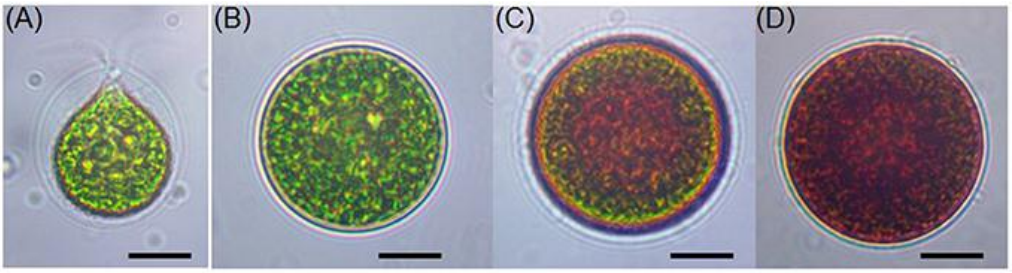

[Figure adapted from Shah M (2016). "Astaxanthin-Producing Green Microalga *Haematococcus pluvialis*: From Signal Cell to High Value Commercial Products". Frontiers in Plant Science, 7 531.]

Figure 1. The microscope images of astaxanthin accumulation process in H. pluvialis cells

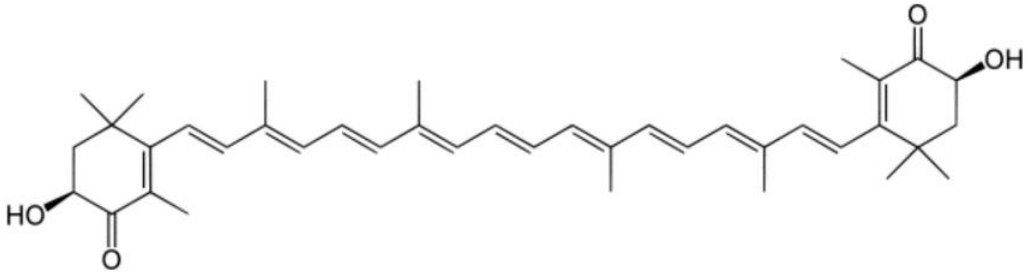

Figure 2. Chemical structure of astaxanthin

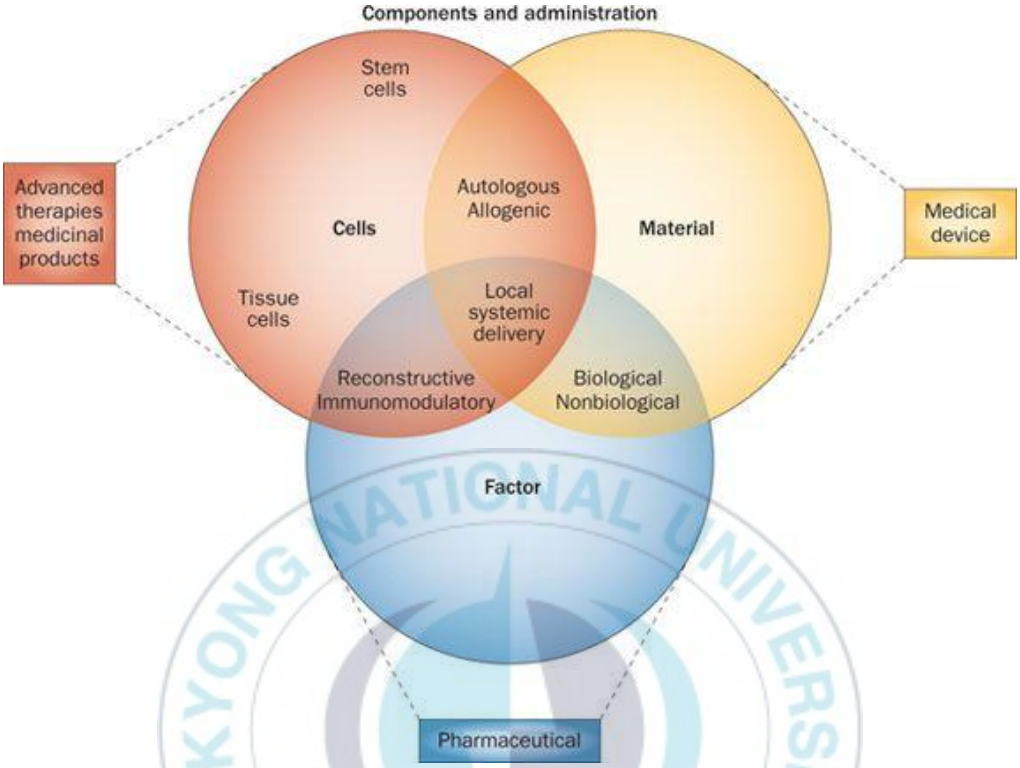

[Figure adapted from Ringe J (2012). "Regenerative medicine in rheumatic disease-progress in tissue engineering". Nature Reviews Rheumatology, 8(8).]

Figure 3. Summary of tissue engineering and regenerative medicine

2. Materials and methods

2.1. Cell culture with astaxanthin reagent

Astaxanthin (3, 3'-dihydroxy-β, β-carotene-4, 4'-dione) derived from the algae *Haematococcus Pluvialis* (Sigma-Aldrich, MO, IL, USA) was dissolved in dimethyl sulfoxide (DMSO) [37]. A stock solution of astaxanthin were prepared and filtered with 0.22 μm nylon membrane filter (Jet biofil, Guangzhou, China). Further, astaxanthin at various concentration were studied *in vitro* for cell proliferation. Rabbit adipose-derived mesenchymal stem cells (Cyagen, Guangdong, China) were cultured in a basal culture medium of Dulbecco's Modified Eagle's medium (DMEM), supplemented with 4.5g/L glucose, L-glutamine, sodium pyruvate, 10% fetal bovine serum (FBS), 1% penicillin-streptomycin, and 1% non-essential amino acids in 5% CO_2 incubator at 37 ℃. All experiments were performed with 5-6 passage number of ADMSCs.

2.2. GelMA synthesis

Briefly, a 10% (w/v) gelatin solution of type A (porcine, Bloom strength ~300, Sigma-Aldrich, USA) was dissolved in Dulbecco's phosphate buffered saline (PBS) at 50 ℃. In addition, methacrylic anhydride (Sigma-Aldrich, MO, IL, USA) was added to gelatin solution at 50 ℃. After rigorous mixing for 1 hour, the reaction was stopped with PBS (5×). The suspension was then dialyzed using 14kDa molecular-weight-cutoff (MWCO) membrane (Sigma-Aldrich, MO, IL, USA) at 40 ℃ for 5 days against

ultrapure water to remove the by-products. The samples were lyophilized for 3-4 days and stored at -20 ℃ until further use [10]. 5% of GelMA were used in all experiments.

2.3. Fabrication of GelMA scaffolds with mesenchymal stem cells

The cultured adipose-derived mesenchymal stem cells were trypsinized- 0.25%, counted, and spun down. The pellets were mixed with 5% of GelMA pre-solution and 0.5% (w/v) photoinitiator of Irgacure 2959 (Sigma-Aldrich, MO, IL, USA) which were sterilized with 0.22 μm polyethersulfone (PES) membrane syringe filter (Jet biofil, Guangzhou, China). Finally, the mixture was crosslinked through a 365 nm ultraviolet (UV) lamp (Thorlabs, USA) with a light intensity of 2.7 mW/cm^2 for 1 min and washed 2 times with PBS.

2.4. Alamar blue assay

To assess cellular proliferation at 1, 2, and 3 days, the alamar blue reagents (Invitrogen, Carlsbad, CA, USA) was used in two-dimensional and three-dimensional cultures. A 10% alamar blue reagent was directly added to the samples with astaxanthin and without astaxanthin for 4 hours. Using a UV-Vis spectrophotometer (BioTek, Winooski, VT, USA), absorbances were measured at 570 nm and 600 nm. All proliferation assays were demonstrated in at least three separate experiments for each day. The percent reduction of alamar blue was calculated using following equation:

$$\text{Percentage reduction } (\%) = \left(\frac{(O2 \times A1) - (O1 \times A2)}{(R1 \times N2) - (R2 \times N1)}\right) \times 100$$

Where, Q1: The molar extinction coefficient (E) of oxidized alamar blue at 570 nm; Q2: E of the oxidized alamar blue at 600 nm; R1: E of the reduced alamar blue at 570 nm; R2: E of reduced alamar blue at 600 nm; A1: Absorbance of test wells at 570 nm; A2: Absorbance of test wells at 600 nm; N1: Absorbance of negative control (without cells) at 570 nm; N2: Absorbance of negative control (without cells) at 600 nm.

2.5. RNA extraction and RT-PCR

After 24 hours exposure of ADMSCs with 0 and 0.5 ng/ml of astaxanthin, the total RNA was isolated from ADMSCs using TRI regent (Sigma-Aldrich, MO, IL, USA). The total RNA concentration was measured using UV/Vis-spectrophotometry (BioTek, Winooski, VT, USA) at 260 nm. cDNA was synthesized from the RNA using the reverse transcription method PrimeScript 1st strand cDNA Synthesis Kit (Takara, Shiga, Japan). Template DNA was then used in gene-specific PCR, wherein synthesized cDNA using oligo-dT primer was amplified by 40 cycles (initial denaturation, denaturation, annealing, and extension: 98 , 1 min, 98 , 10 sec; 55-60 , 30 sec; 72 , 1 min). The expression of stemness-related genes (SOX2 and KLF4 (Bioneer, Alameda, California, USA)) and the proliferation-related genes (Rex1, c-MCY, and Wnt3a (Bioneer, Alameda, California, USA)) were tested, wherein Glyceraldehyde 3-phosphate dehydrogenase (GAPDH) was used as a housekeeping gene. Details of the primers are listed in (Table 1). Further, aliquots of PCR product were electrophoresed

onto 1.5% agarose gels, PCR fragments were stained with loading STAR dye (Dynebio, Gyeonggi-do, South Korea) and visualized under UV light using the gel documentation system (Daihan Scientific, Seoul, South Korea). All gene expression experiments were tested in triplicates.

2.6. Proton nuclear magnetic resonance

The lyophilized GelMA materials with and without astaxanthin were dissolved into deuterium oxide (D_2O) solution at 40 . The methacrylation degree of the free amine group in the GelMA materials were analyzed by the Fourier transform nuclear magnetic resonance spectrometer JNM ECP-600 MHz (JEOL, Tokyo, Japan). The data were processed using JEOL delta V5.3 software (JEOL, Tokyo, Japan) and the degree of methacrylation was calculated [11].

$$\text{Methacrylation degree (\%)} = \left(1 - \frac{\text{Lysine integration signal of GelMA}}{\text{Lysine integration signal of geltain}}\right) \times 100$$

2.7. Physical characterization

To analyze the mechanical property of GelMA and astaxanthin-incorporated GelMA hydrogels, a dynamic rheological was performed using a rheometer (Discovery HR-2, TA instrument, USA) equipped with 8 mm parallel plate. Using UV light, crosslinked samples were loaded into a 1 mm gap. Firstly, to determine the linear viscoelasticity region, strain amplitude sweeps (0.01-100%) were performed. A time sweep test was

set at an angular frequency of 10 rad/s for 300s to show the time-dependent stability of the material. The frequency sweep test was demonstrated at an angular frequency of 0.1-100 rad/s at a strain in the linear viscoelastic ranging to protect against destroying the structure of the samples. All tests were performed at 25 with fixed strain of 1%, except the temperature ramp test, which ranged between 45 to 25 and demonstrated in triplicate [15].

For mechanical characteristics and the diffusion process, the hydrogels were lyophilized under dry conditions and were weighed (W_d). The dried hydrogels were then immersed in PBS, incubated at 37 and weighed (W_s). The swelling ratio was calculated under this formula:

$$\text{Swelling ratio } (\%) = \frac{(Ws - Wd)}{Wd} \times 100$$

Where, W_d is the dry weight of hydrogels, W_s is the weight of swollen hydrogel.

2.8. Confocal imaging of live/dead staining

To study qualitative analysis and morphological changes of cellular proliferation in encapsulated hydrogel with and without astaxanthin, live/dead staining was performed. Briefly the hydrogels were incubated in fluorescein diacetate (FDA, Sigma-Aldrich, USA) and propidium iodide (PI, Sigma-Aldrich, USA) dyes for 6 min at room temperature and were then washed with PBS thrice. Confocal laser scanning microscope system A1+ (Nikon, Tokyo, Japan) at 100× magnification was used to

scan all three-dimensional images. The live/dead images processed to Z-projection and volume by the ImageJ software (V1.8, NIH, Bethesda, MD, USA) and a NIS-Elements viewer V4.50 software (Nikon, Japan).

2.9. Statistical analysis

Data were reported as mean ± standard deviation and analyzed for statistical significance by ANOVA test using IBM SPSS Statistics Version 12 software (Chicago, IL, USA). Analytical methods mainly included descriptive analysis.

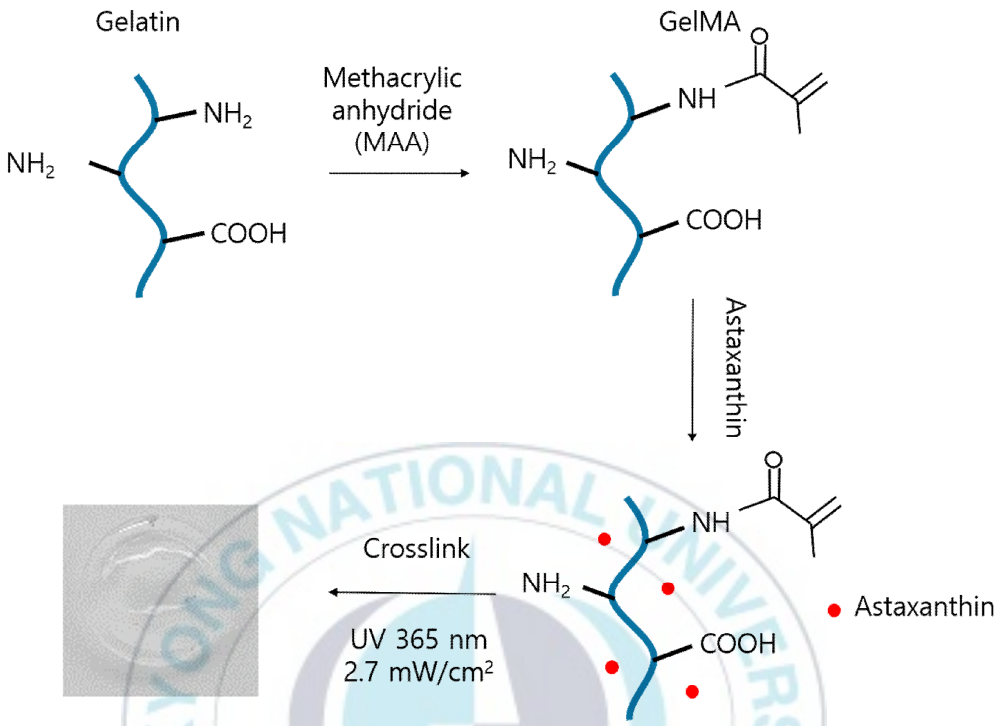

Figure 4. Schematic image of the fabrication process of astaxanthin incorporated in GelMA hydrogel.

Table. 1 Primer sequences used for RT-PCR.

Symbol	Forward	Reverse
SOX2	GGCGGCAACCAGAAGAACAG	TCGAGAACGGCCGCTTCTC
KLF4	AGCCCCAAGATGCACAACTC	AGGACGAGGAAGAGGCAGAC
Wnt3a	TTCCTCAAGGACAAGTACGACA	GAAGTTGGGGGAGTTCTCATAG
Rex1	AGCCCAGCAGGCAGAAATGGAA	TGGTCAGTCTCACAGGGCACAT
c-MYC	TCGGACTCTCTGCTCTCCTC	CTTGTCGTTCTCCTCGGTGT
GAPDH	CAAGTTCCACGGCACGGTCA	CTCGGCACCAGCATCACCC

3. Results and discussion

3.1. Cellular proliferation assay in two-dimensional environments

To access the effect of various concentrations of astaxanthin (0, 0.5, 5, 50, and 500 ng/ml) on cellular proliferation, alamar blue assay was performed in figure. 5. The proliferation of the mesenchymal stem cells was increased after in a time-dependent manner. Specially, the ADMSCs in the concentration of 0.5 ng/ml indicated the highest proliferation. In cellular proliferation, the higher concentrations (500 ng/ml) decreased with time. In addition, microscopy images of ADMSCs were treated with various astaxanthin concentrations was showed to support quantitative results in figure. 6. The images observed that an increase in cell number was confirmed with healthy spindle shaped cells in the concentration of 0.5 ng/ml compared to concentration of 0 ng/ml. In high concentrations (50 and 500 ng/ml) was shown lower cell numbers than the concentration of 0 and 0.5 ng/ml. Astaxanthin concentrations of 0.5 ng/ml was selected as the optimal concentrations for further experiments.

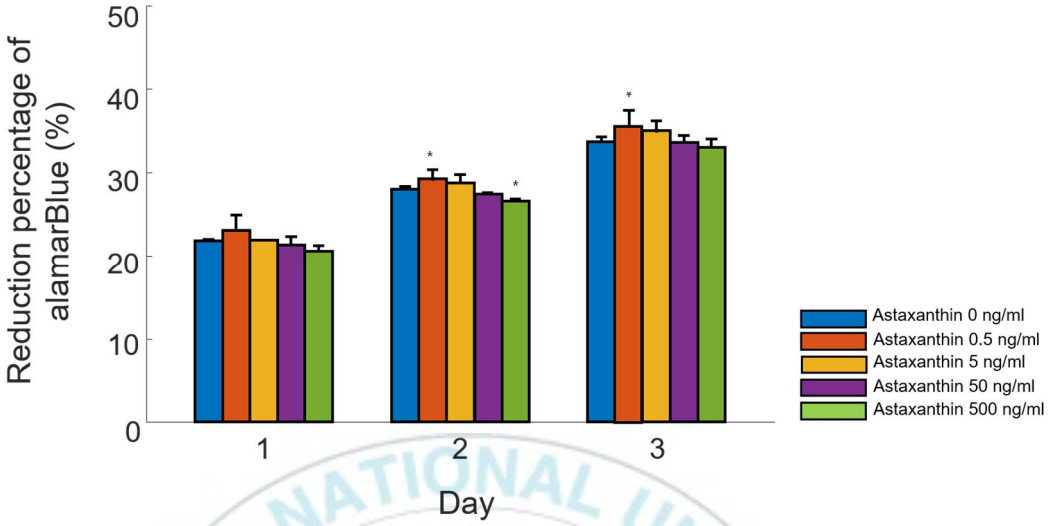

Figure 5. Proliferation of ADMSCs treated with different concentrations of astaxanthin on day 1, 2, and 3 days were performed by alamar blue assay.

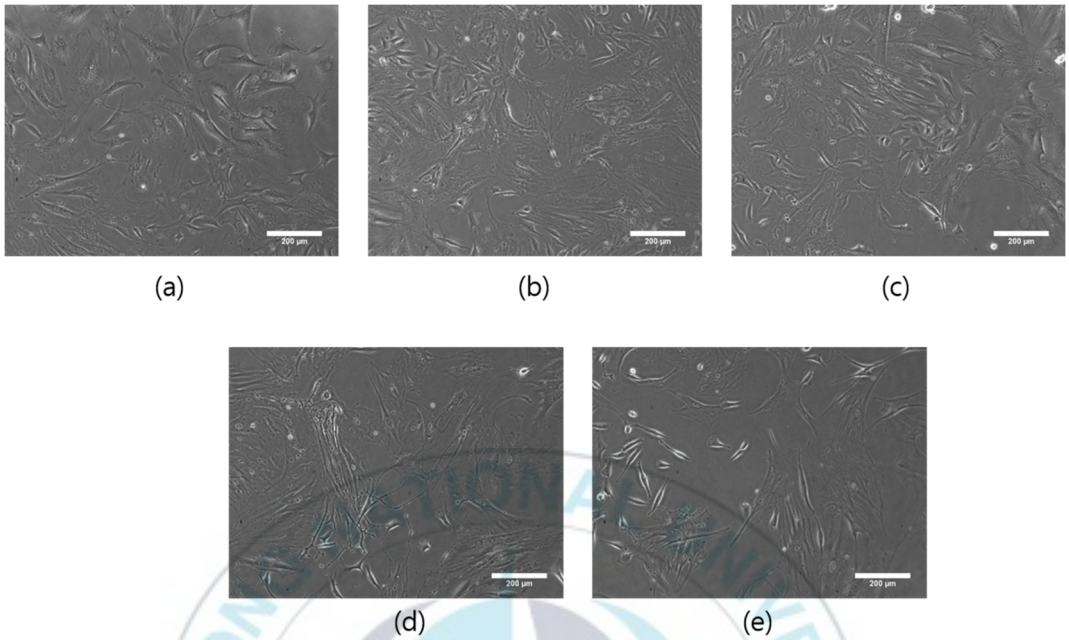

Figure 6. Optical microscopy images of adipose derived mesenchymal stem cells treated astaxanthin at various concentrations of (a) 0 ng/ml, (b) 0.5 ng/ml, (c) 5 ng/ml, (d), 50 ng/ml, and (e) 500 ng/ml. (scale = 200 μm).

3.2. Reverse transcription polymerase chain reaction (RT-PCR)

In various other research, multiple antioxidants such as N-acetyl-L-cysteine, L-ascorbic acid 2-phosphate, and sulforaphane was demonstrated for positive influences on cellular proliferation, as well as stemness of stem cells [23,24,25]. Antioxidants can improve genomic stability and also promote proliferation by raising the number of cells in the S phage of the ADMSCs [26]. To prove the influence of astaxanthin as antioxidant materials on the proliferation of ADMSCs, reverse transcription-PCR for the expression of molecular marker including proliferation-related transcription factors and stemness genes was performed. In figure. 7, the treatment of astaxanthin in the concentration of 0.5 ng/ml was shown upregulated expression of stemness genes (SOX2 and KLF4) and proliferation-related transcription factors (Rex1, c-MYC, and Wnt3a) on one day [5]. In particular, the Sox2 gene was markedly over expressed, which is known for its role in the maintenance of pluripotency [27]. c-MYC, known to regulate the self-renewal capacity of stem cells was also upregulated. Rex1 is highly essential aspect of keeping proliferation in mesenchymal stem cells through the suppression of p39 MAPK signaling via the direct suppression of MKK3 [28]. Expression of Rex1 was increased because of the increased proliferation in ADMSCs treated with 0.5 ng/ml of astaxanthin. Wnt3a was also upregulated, which shown that cellular proliferation was improved through the wingless-related integration site (Wnt) signaling pathway [29]. KLF4 genes, a direct target of the MAPK signaling pathway, promotes the stemness of stem cells for self-renewal. Therefore, astaxanthin can enhance cellular proliferation and maintain self-renewal was shown in these results.

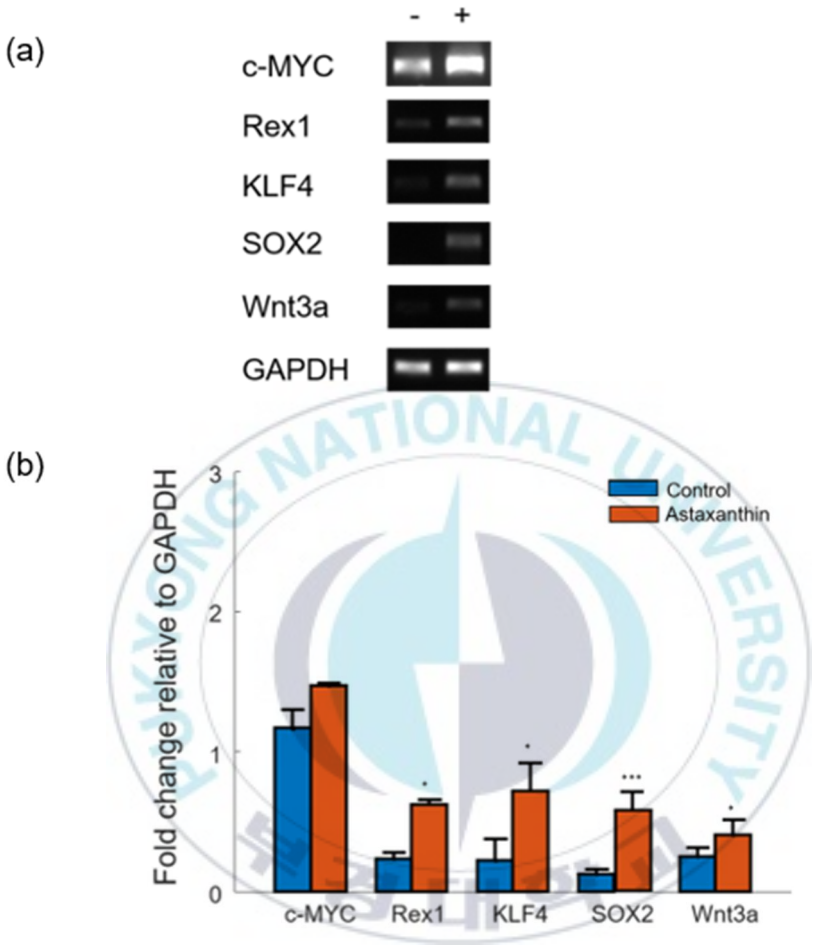

Figure 7. (a) Gene expression of 0.5 ng/ml of astaxanthin related proliferation and cell renewal. and (b) Quantified gene expression in bar graph normalized to GAPDH. Data are processed as the mean ± standard deviation (n=3).

3.3 Chemical characterization of astaxanthin incorporated GelMA

The degree of substitution of free amino groups in samples can be controlled by the amount of methacrylic anhydride and the reaction times for photopolymerization. The peaks of the synthesized hydrogen atoms in methacrylate group was confirmed by the proton nuclear magnetic resonance (^{1}H NMR).

For quantification of the degree of substitution, the spectra were normalized to the phenylalanine signal (7.0-7.5 ppm), which contains the concentrations of gelatin. New peaks (5.5 and 5.8 ppm) appeared in the spectrum of GelMA comparing to that of gelatin, which shows the acrylic protons (2H) of methacrylic methacryloyl functions in figure. 8. The peaks of GelMA with and without astaxanthin shown in box C and were corresponded to the methylene protons (2H) of unreacted lysine groups (3.1 ppm) and were slightly decreased compare to that of gelatin. Moreover, in box D, the peak was observed only in GelMA with astaxanthin (2.7-2.8 ppm), indicating the presence of astaxanthin [30,31]. The peaks in box E (1.98 ppm) for the methyl protons (3H) groups of methacrylamide grafts show methacrylation in GelMA. The phenylalanine peaks (7.0-7.5 ppm) were set as the internal reference to normalize the amine signals (3.1 ppm) of methacrylated lysine. The degree of substitution with methacrylate group in this study was 56.65% yield by the ^{1}H NMR spectrum [11,32,33]. Therefore, these results elucidated that the methacrylate groups and methacrylamide groups have been successfully grafted to the gelatin as presented in box A+B, C, and E well incorporated with astaxanthin in GelMA as shown in box D.

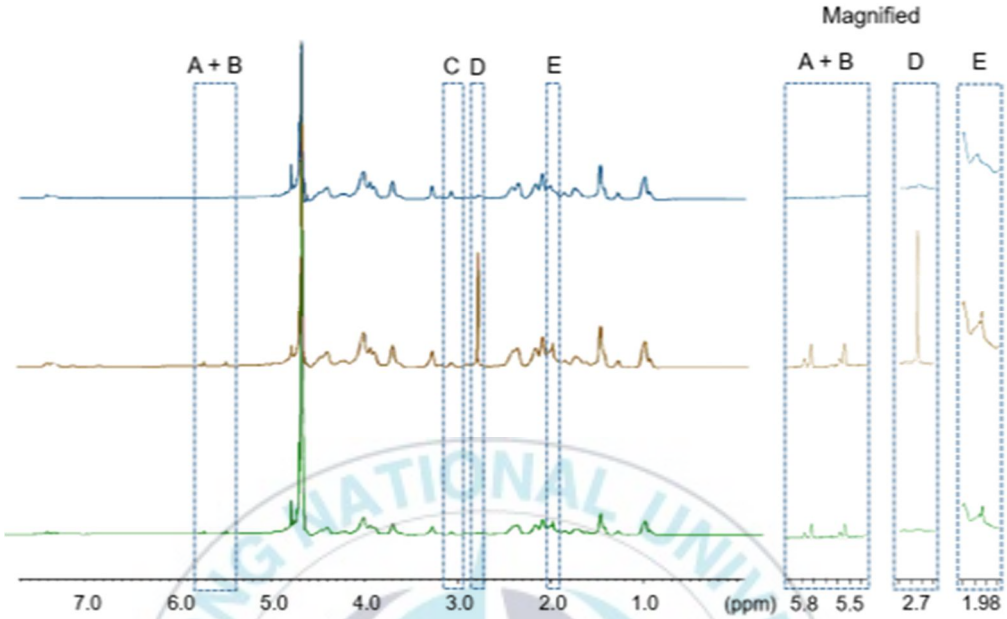

Figure 8. H-NMR spectra of gelatin only, GelMA only, and GelMA incorporated with astaxanthin in D2O. Box A+B-acrylic protons (2H) of methacryloyl functions. Box C-methylene protons (2H) of non-modified lysine groups. Box D-astaxanthin peaks. Box E-methyl protons (3H) groups of methacryloyl groups.

3.4. Rheological analysis of astaxanthin incorporated GelMA

For choosing the linear viscoelastic region, strain amplitude sweeps (0.01-100%) were first performed before the measurement of storage moduli. A time-sweep test was tested to confirm that the material is maintaining its time-stable form for five minutes. In figure. 9, all of the samples maintained its storage moduli in the time-dependent test. The storage moduli of GelMA samples with and without astaxanthin slightly decrease because of the temperature increases (red and green) in the temperature-dependent rheological test. However, the storage modulus gelatin (blue) which is thermo-sensitive polymer was dramatically reduced over 30 [16]. These results indicated that GelMA-based hydrogels holding-up gradient temperature better comparing gelatin hydrogels due to more robust networking of crosslinking. In a frequency sweep test, GelMA showed slightly decreased storage moduli (G') frequency range possibly because of the scavenging property of astaxanthin thereby decrease free radicals generation.

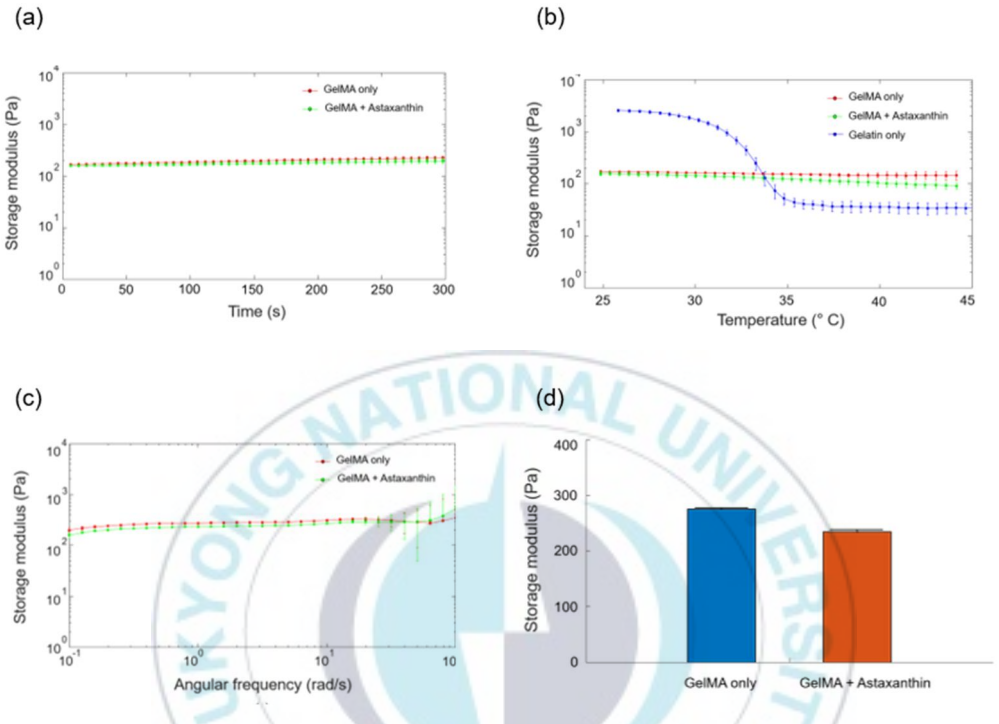

Figure 9. Rheological analysis of GelMA with and without astaxanthin (a) Time sweep test, (b) temperature ramp test, (c) frequency sweep test, and (d) the values of storage moduli (G') at the frequency of 1 rad/s. Data are processed as the mean ± standard deviation (n=3).

3.5. Swelling properties

In hydrogel, the swelling behavior is an important in tissue engineering, since it affects various parameters including surface properties, mobility and solute diffusion. The swelling ability of GelMA with astaxanthin (red) and without astaxanthin (black) are shown in figure. 10. GelMA with astaxanthin revealed a more increased swelling ratio comparing control. In particular, the swelling ratio of all samples increased during the initial 1 h. After 5 hours of immersion, all samples nearly reached an equilibrium in figure. 10b. This can be attributed to the antioxidant property of astaxanthin, wherein the ratio of radical polymerization of the macromers was reduced by scavenging the radical formed, as the demonstrated by Chiellini et al [35]. The experimental results may elucidate astaxanthin which has distinguished groups possibly scavenges the free radicals in GelMA, which can make a result of slightly increase of water absorption.

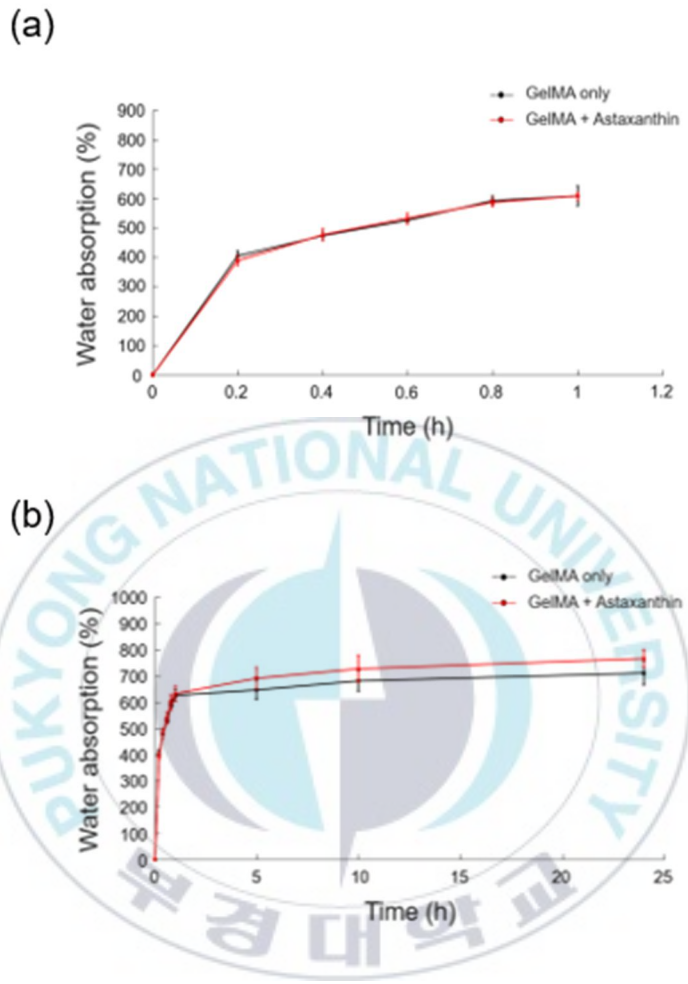

Figure 10. The swelling behaviors of GelMA with astaxanthin (red) and without astaxanthin (black). (a) from 0 to 1 hour and (b) from 0 to 24 hours. Data are processed as the mean ± standard deviation (n=3).

3.6. Cellular proliferation and viability in astaxanthin-incorporated GelMA scaffolds.

The cellular proliferation of adipose-derived mesenchymal stem cells cultured in GelMA hydrogels with astaxanthin (0.5 ng/ml and 50 ng/ml) and without astaxanthin (control) on day 1, 4, and 7 in figure. 11 was shown by the alamar blue assay. The control graph indicates an increase in cellular proliferation over time, which means non-toxicity and a cellular attachment of GelMA-based scaffolds. Compared to our control, astaxanthin incorporated into GelMA improved the cellular proliferation of ADMSCs on day 4 for both concentrations (0.5 ng/ml and 50 ng/ml). On day 7, however, a slight dip was showed in 50 ng/ml of astaxanthin, which could be overdosed to promote cellular proliferation. ADMSCs encapsulated in GelMA-based hydrogels also reflected that 0.5 ng/ml of astaxanthin was the optimal concentration at different time points are performed in the two-dimensional cells culture experiment.

Qualitative analysis of the cellular viability with and without the interaction with astaxanthin, was performed by using live/dead staining using laser confocal microscopy after 8 days. The dimensions of all samples are 10 mm and 22 mm (in diameter and height). The scanning area of the confocal microscope are width 1272.79 μm, depth 276 μm, and 1272.79 μm, respectively. The first row of the images of figure. 12 clearly shows that ADMSCs thrived in both the hydrogels and photo-induced crosslinking treatment of the hydrogel did not cause any significant deleterious effects on cellular viability. There is evident increase in the number of cells with an even spread in the GelMA hydrogels with astaxanthin compared to control without astaxanthin.

Obviously, ADMSCs treated with astaxanthin showed more robust cell morphology with elongation. Furthermore, more filopodia were observed in figure. 12b, indicating an early interconnected network of cells within the hydrogel. Also, for the following other experiments, major carotenoid materials like astaxanthin, carotene, lutein, zeaxanthin and lycopene stimulate gap junctional intercellular communication, changing the phosphorylation pattern of connexin [35,36]. This could be attributed to the presence of astaxanthin in a three-dimensional hydrogel which induces improved cell-cell communication, thus exhibiting an advantageous feature in three-dimensional scaffolds that mimics in vivo environments [18,19].

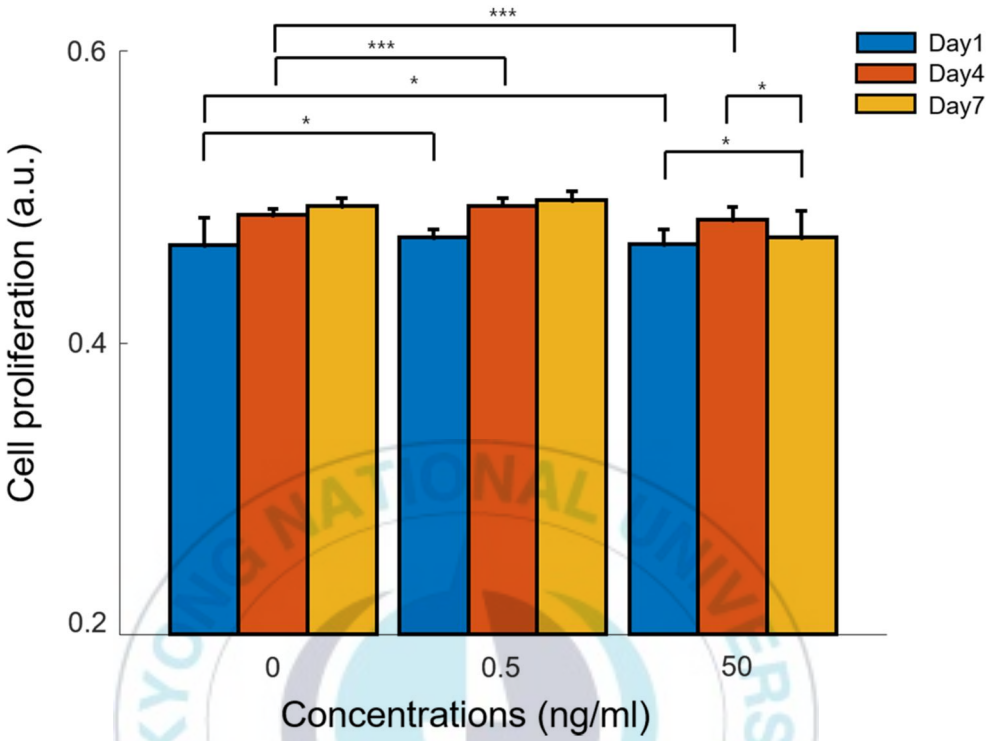

Figure 11. Cellular proliferation in three-dimensional GelMA-based hydrogels with different concentrations of astaxanthin (0, 0.5, and 50 ng/ml) on day 1, 4, and 7. Data are processed as the mean ± standard deviation (n=3).

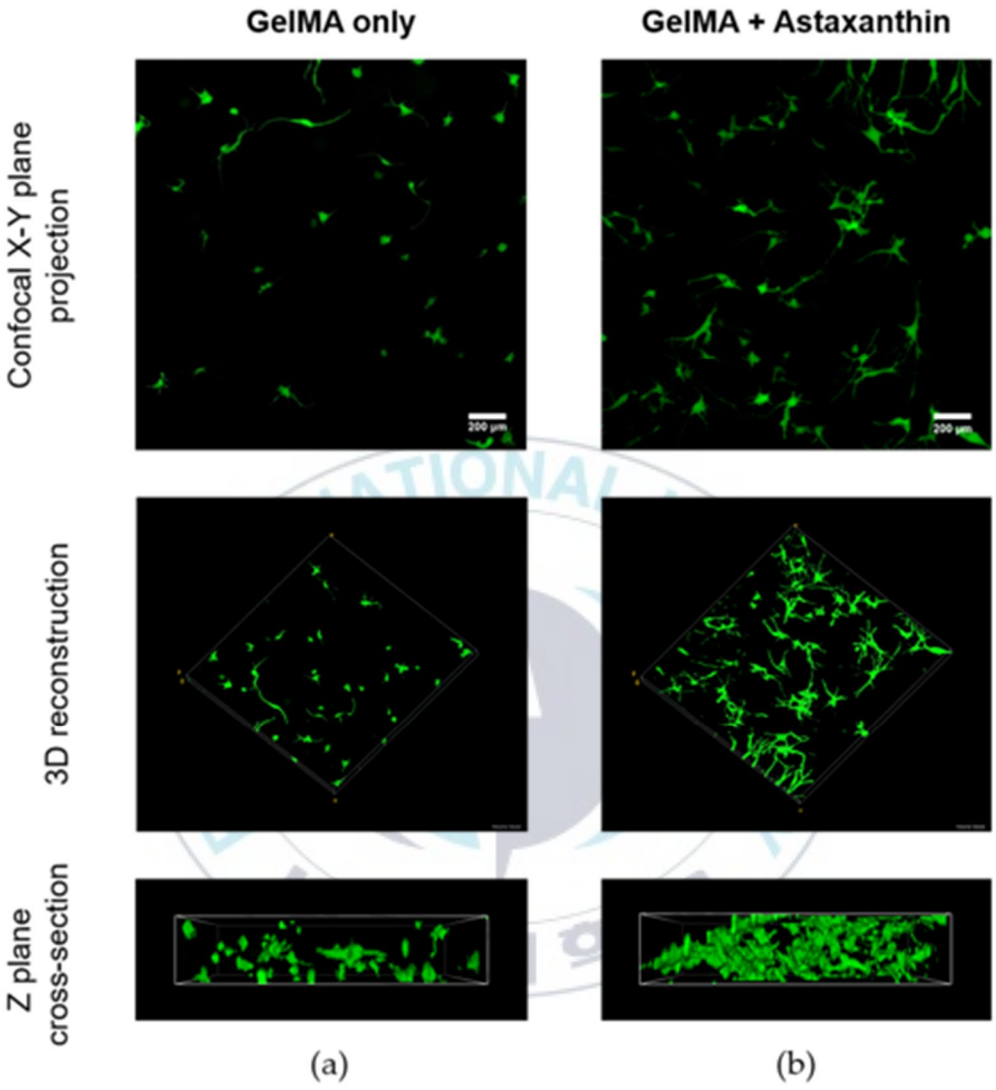

Figure 12. Confocal images of ADMSCs in GelMA (a) and incorporated astaxanthin (b) using live/dead staining after 8 days. (scale bar = 200 μm)

4. Conclusion

The results of this study demonstrated astaxanthin had a positive impact upon the cellular proliferation of adipose-derived mesenchymal stem cells by alamar blue assay in a time-dependent. The results corresponding to the alamar blue assay carried out in overexpressed proliferation-related genes and stemness genes.

Moreover, it confirmed that astaxanthin was successfully incorporated in the GelMA scaffolds and showed the feasibility of encapsulated GelMA hydrogels with astaxanthin to improve cell-cell networking through physico-chemical characterization and biological analysis of hydrogels. Thus, the addition of astaxanthin promises to induce stem cell potency via proliferation, and it can be a useful tool for tissue engineering and regenerative medicine applications.

5. Future study

One of dynamic tissues is bone tissue that support body weight, protect organs and regulate homeostasis of inorganic substance. Bone regeneration which is the concern of many people requires materials capable of providing mechanical and chemical signals to increases biomineralization [38]. Bioactive materials have become gradually useful as a new generation of biomaterials.

In this study, astaxanthin had a positive impact upon the cellular proliferation of adipose-derived mesenchymal stem cells. It has also been shown that astaxanthin can enhance the differentiation of stem cells including neural stem cells, adipose-derived mesenchymal stem cells into chondrocytes, osteoblasts, and adipocytes [4, 7-9].

We also confirmed the potential of astaxanthin to enhance differentiation of adipose-derived mesenchymal stem cells into osteogenic lineage through alkaline phosphatase (ALP), real-time qPCR, alizarin red staining (ARS) assay in figure. 13. In future study, tissue engineered constructs combined with astaxanthin can be fabricated using various methods such as coaxial bioprinting, coating, and soaking to enhance osteoconductivity.

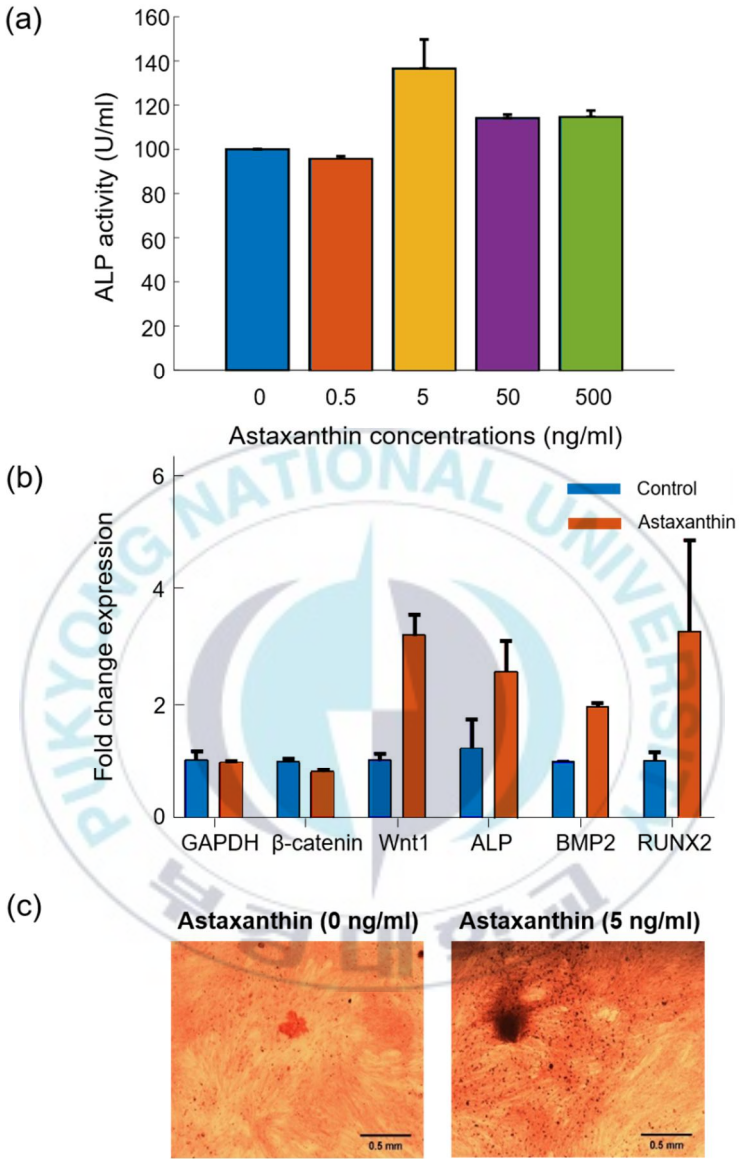

Figure 13. The effect of astaxanthin on osteogenic differentiation in adipose-derived mesenchymal stem cells (a) alkaline phosphatase activity, (b) expression of osteogenic marker by RT-qPCR, and (c) mineralization by alizarin red-s. (scale bar = 500 μm)

6. References

[1] Zhang, X., Kim G., Kang, M., Lee, J., Seo, J., Do, j., Hong, K., Cha, J., Shin, S., and Bae, H., (2018). "Marine biomaterial-based bioinks for generating 3D printed tissue constructs." Marine Drugs 16: 484.

[2] Fakhri, S., Abbaszadeh, F., Dargahi, L., and Jorjani, M. (2018). "Astaxanthin: A mechanistic review on its biological activities and health benefits." Pharmacological Research 136: 1-20.

[3] Ambati, R., Phang, S.-M., Ravi, S., Aswathanarayana, R (2014). "Astaxanthin: Sources, extraction, stability, biological activities and its commercial applications-A review." Marine Drugs 12: 128-152.

[4] Kim, J.H., Nam, S.-W., B.W., Kim, W.-J., and Choi, Y.H. (2010). "Astaxanthin improves the proliferative capacity as well as the osteogenic and adipogenic differentiation potential in neural stem cells." Food and Chemical Toxicology 48: 1741-1745.

[5] Kim, J.H., Nam, S.-W., Kim, B.-W., Choi, W., Lee, J.-H., Kim, W.-J, and Choi, Y.-H (2010). "Astaxanthin improves stem cell potency via an increase in the proliferation of neural progenitor cells." International Journal of Molecular Sciences 11: 5109-5119.

[6] Choi, B.Y., Chalisserry, E.P., Kim, M.H., Kang, H.Y, Choi, I.-H, and Nam, S.Y. (2019). "The influence of astaxanthin on the proliferation of adipose-derived mesenchymal stem cells in gelatin-methacryloyl (GelMA) hydrogels." Materials 12(15): 2416.

[7] Ghasemi, N., (2018). "The evaluation of astaxanthin effects on differentiation of human adipose-derived stem cells into oligodendrocyte precursor cells." Avicenna Journal of Medical Biotechnology 10: 69-74.

[8] Yaghooti, H., Mohammadtaghvaei, N., and Mahboobnia, K. (2019). "Effects of palmitate and astaxanthin on cell viability and proinflammatory characteristics of mesenchymal stem cells." International Immunopharmacology 68: 164-170.

[9] Zhang, J. and Peng, C.-A., (2019). "Enhanced proliferation and differentiation of mesenchymal stem cells by astaxanthin-encapsulated polymeric micelles." PLoS ONE 14: e0216755.

[10] Loessner, D., Meinert, C., Kaemmerer, E., Martine, L.C., Yue, K., Levett, P.A., Klein, T.J., Melchels, F,P., Khademhosseini, A., and Hutmacher, D.W. (2016).

"Functionalization, preparation and use of cell-laden gelatin methacryloyl-based hydrogels as modular tissue culture platforms." Nature Protocols 11: 727.

[11] Kim, H., Bae. C., Kook, Y-M., Koh, W-G., Lee, K., and Park, M.H. (2019). "Mesenchymal stem cells 3D encapsulation technologies for biomimetic microenvironment in tissue regeneration." Stem Cell Research & Therapy 10: 51.

[12] Wang, Z., Tian, Z., Menard, F., and Kim, K. (2017). "Comparative study of gelatin methacrylate hydrogels from different sources for biofabrication application." Biofabrication 9: 044101.

[13] Nichol, J.W., Koshy, S.T., Bae, H., Hwang, C.M., Yamanlar, S., and Khademhosseini, A. (2016). "Cell-laden microengineered gelatin methacrylate hydrogels." Biomaterials 31: 5536-5544.

[14] Lai, T., Yu, J., and Tsai, W. (2016). "Gelatin methacrylate/carboxybetaine methacrylate hydrogels with tunable crosslinking for controlled drug release." Journal of Materials Chemistry 4.13: 2304-2313.

[15] Billiet, T., Gevaert, E., De Schryver, T., Cornelissen, M., and Dubruel, P. (2014). “The 3D printing of gelatin methacrylamide cell-laden tissue-engineered constructs with high cell viability." Biomaterials 35: 49-62.

[16] Lee, B., Lum, N., Seow, L., Lim, P., and Tan, L. (2016). “Synthesis and characterization of types a and b gelatin methacryloyl for bioink applications” Materials, 6: 797.

[17] Wang, X., Ao, Q., Tian, X., Fan, J., Tong, H., Hou, W., and Bai, S. (2017). "Gelatin-based hydrogels for organ 3D bioprinting." Polymers 9: 401.

[18] Bahney, C., Lujan, T., Hsu, C., Bottlang, M., West, J., and Johnstone, B., (2011). "Visible light photoinitiation of mesenchymal stem cell-laden bioresponsive hydrogels." eCells & Materials Journal 22: 43.

[19] Lin, C. H., Su, J.J.M., Lee, S.Y., and Lin, Y.M. (2018). "Stiffness modification of photopolymerizable gelatin-methacrylate hydrogels influences endothelial differentiation of human mesenchymal stem cells." Tissue engineering and regenerative medicine 12: 2099-2111.

[20] Pepelanova, I., Kruppa, K., Scheper, T., and Lavrentieva, A. (2018). "Gelatin-Methacryloyl (GelMA) hydrogels with defined degree of functionalization as a versatile toolkit for 3D cell culture and extrusion bioprinting." Bioengineering 5: 55.

[21] Zuk, P. A., Zhu, M., Mizuno, H., Huang, J., Futrell, J.W., Katz, A.J., Benhaim, P., Lorenz, H.P., and Hedrick, M.H. (2001). "Multilineage cells from human adipose tissue: Implications for cell-based therapies." Tissue Engineering 7: 211-228.

[22] Konno, M., Hamabe, A., Hasegawa, S., Ogawa, H., Fukusumi, T., Nishikawa, S., Ohta, K., Kano, Y., Ozaki, M., and Noguchi, Y. (2013). "Adipose-derived mesenchymal stem cells and regenerative medicine." Development, Growth & Differentiation 55: 309-318.

[23] Sun, L.-Y, Pang, C.-Y., Li, D.-K., Liao, C.-H., Huang, W.-C., Wu, C.-C., Chou, Y.-Y., Li, W.W., Chen, S.-Y., and Liu, H.-W. (2013). "Antioxidants cause rapid expansion of human adipose-derived mesenchymal stem cells via CDK and CKD inhibitor regulation." Journal of Biomedical Science 20: 53.

[24] Marrazzo, P., Angeloni, C., Freschi, M., Lorenzini, A., Prata, C., Maraldi, T., and Hrelia, S. (2018). "Combination of epigallocatechin gallate and sulforaphane counteracts in vitro oxidative stress and delays stemness loss of amniotic fluid stem cells." Oxidative Medicine and Cellular Longevity 2018: 13.

[25] Yu, j., Tu., Y.-K., Tang, Y.-B., and Cheng, N.-C. (2014). "Stemness and transdifferentiation of adipose-derived stem cells using L-ascorbic acid 2-phosphate-induced cell sheet formation." Biomaterials 35: 3516-3526.

[26] Shaban, S., El.-Husseny, M.W.A., Abushouk, A.I., Salem, A.M.A., Mamdouh, and M., Abdel-Daim, M.M. (2017). "Effects of antioxidant supplements on the survival and differentiation of stem cells." Oxidative Medicine and Cellular Longevity 207: 16.

[27] Park, S., Seo, K.W., So, A., Seo, M., Yu, K., Kang, S., and Kang, K. (2012). "SOX2 has a crucial role in the lineage determination and proliferation of mesenchymal stem cell through Dickkopf-1 and c-MYC." Cell Death Differentiation 19: 534.

[28] Bhandari, D.R., Seo, K.-W., Roh, K.-H., Jung, J.-W., Kang, S.-K., and Kang, K.-S. (2010). "REX-1 expression and p38 MAPK activation status can determine proliferation/differentiation fates in human mesenchymal stem cells." PLoS ONE 5: e10493.

[29] Boland, G.M., Perkins, G., Hall, D.J., and Tuan, R.S. (2004). "Wnt 3a promotes proliferation and suppresses osteogenic differentiation of adult human mesenchymal stem cells." Journal of Cellular Biochemistry 93: 1210-1230.

[30] Holtin, K., Kuehnle, M., Rehbein, J., Schuler, P., Nicholson, G., and Albert, K. (2009). "Determination of astaxanthin an astaxanthin esters in the microalgae Haematococcus pluvialis by LC-(APCL) MS and characterization of predominant

carotenoid isomers by NMR spectroscopy." Analytical and Bioanalytical Chemistry 395: 1613.

[31] LaFountain, A.M., Pacheco, C., Prum, R.O., and Frank, H.A. (2013). "Nuclear magnetic resonance analysis of carotenoids from the burgundy plumage of the Pompadour Cotinga (Xipholena punicea)." Archives of Biochemistry and Biophysics 539: 133-141.

[32] Zhu, M., Wang, Y., Ferracci, G., Zheng, J., Cho, N.-J., and Lee, B.H. (2019). "Gelatin methacryloyl and its hydrogels with an exceptional degree of controllability and batch-to-batch consistency." Scientific Reports 2019: 9.

[33] Wang, Y., Ma, M., Wang, J., Zhang, W., Lu, W., Gao, Y., Zhang, B., and Guo, Y. (2018). "Development of a photo-crosslinking, biodegradable GelMA/PEGDA hydrogel for guided bone regeneration materials." Materials 11: 1345.

[34] Chiellini, F., and Morelli, A. (2011). "Ulvan: A versatile platform of biomaterials from renewable resources." Biomaterials-Physics and Chemistry 75-98.

[35] Daubrawa, F., Sies, H., and Stahl, W. (2005). "Astaxanthin diminishes gap junctional intercellular communication in primary human fibroblasts." Journal of Nutrition 135: 2507-2511.

[36] Packer, L. (2005). "Carotenoids and Retinoids: Molecular Aspects and Health Issues." Lester Packer, U.O.-J., Kalus, K., Helmut, S., Eds. AOCS Publishing: Champaign, IL, USA.

[37] Song, X., Wang, B., Lin, S., Jing, L., Mao, C., Xu, P., Lv, C., Liu, W., and Zuo, J. (2014). "Astaxanthin inhibits apoptosis in alveolar epithelia cells type in vivo and in vitro through through the ROS-dependent mitochondrial signaling pathway." Journal of Cellular and Molecular Medicine, 18, 2198-2212.

[38] Storrie., and Samuel, I. (2005). "Cellular response to zinc-containing organoapatite: an in vitro study of proliferation, alkaline phosphatase activity and biomineralization." Biomaterials, 26(27), 5492-5499.